PED-Vol. 67/TRIB-Vol. 4, Contact Problems and Surface Interaction
in Manufacturing and Tribological Systems
ASME 1993

A MODEL FOR PREDICTING THE THERMAL CONSTRICTION RESISTANCE IN FRETTING

M. Helmi Attia
Materials Technology Unit
Ontario Hydro Technologies
Toronto, Ontario, Canada

M. M. Yovanovich
Department of Mechanical Engineering
University of Waterloo
Waterloo, Ontario, Canada

ABSTRACT

The prediction of the wear characteristics of a fretting tribo-system requires an analytical capability to estimate the friction-induced temperature rise in the contact zone as a function of the process variables. This can only be achieved, if the division of frictional heat between the contacting solids, and the thermal characteristics of the whole system, e.g., the thermal boundary conditions and the external heat sources, are taken into consideration. Numerical methods, e.g., finite difference and finite element, seem to offer the only approach to model and solve the heat transfer problem in a realistic tribo-system. The main obstacle, which prevents us from applying these methods, is the lack of a model that correlates the thermal constriction resistance at the micro-contact area to the parameters of the fretting process. The objective of the present study is to bridge this gap and to develop such a model. For the range of process variables covered in this paper, it has been concluded that the thermal constriction resistance in fretting is greater than that in static contact. This effect is more pronounced at higher levels of Fourier modulus. It has also been observed that the thermal constriction resistance is nearly constant during the quasi-steady state, and is independent of the amplitude of oscillation and mode of motion. A correlation between the constriction resistance and the process parameters has been established.

INTRODUCTION

Due to the nature of engineering surfaces, the real contact area is a very small fraction of the apparent area of contact. As a result, the friction heat generated at the micro-contact area will spread out rather than taking a straight path. This gives rise to the so-called "thermal constriction (or spreading) resistance R_c". To overcome this microscopic constriction resistance, a steep temperature gradient has to be established in the subsurface layer. The analysis presented in [1] showed that the temperature distribution in the thermally disturbed subsurface layer (in the order of 50-100 m thick) is exponential and may result in a significant rise in the contact temperature. It has been established that the temperature at the contact interface and within the subsurface layer has a decisive influence on the mechanical and chemical aspects of the fretting wear process [2-6]. Since the contact temperature can only indirectly be measured, some theoretical models are needed to extrapolate measurements. The model developed by Attia et al. [1,7,8] to estimate the contact temperature rise assumed that all the frictional heat enters the body that oscillates with respect to the friction-heat sources located at the micro-contact areas.

To predict the response behaviour of a real fretting tribo-system (of a complicated geometry, and realistic thermal boundary conditions), the division of the friction heat, and the thermal characteristic of the whole system should be considered. This can only be achieved by using numerical methods, e.g., finite element and finite difference, similar to the work done to solve the heat transfer process in sliding tribo-systems [e.g., 9-12]. In the analyses presented in [9,10], the thermal constriction resistance R_c for constant, uniform heat flow in static contact was used. Ling and Pu [9] noted, however, that more detailed analysis of R_c is required. The only missing link in adopting this approach is lack of qualitative understanding and quantitative modelling of the thermal constriction phenomenon in fretting. Therefore, the main objective of the present study is to develop a general model for the thermal constriction resistance R_c in fretting, which relates R_c to the process variables, namely, the motion parameters, the material

properties, the mechanical loading, and the characteristic length of the micro-contact area. Since the micro-contact areas are thermally connected in parallel, the analysis of the heat transfer process at a single micro-contact spot constitutes the basic cell for predicting the overall thermal resistance of the interface. The R_c-model developed in this paper takes into consideration the thermal interaction between adjacent micro-contacts, and the finite thermal capacity of the body. This is achieved by solving the heat transfer process in an elemental heat flow channel **HFC**, which encompasses a single micro-contact and extends some distance in the solid [13].

THERMAL CONSTRICTION RESISTANCE R_c IN FRETTING- HFC MODEL

Statement of the Problem

Following Tsukada's approach [14], it is assumed that the contact between two rough surfaces is replaced by a perfectly smooth, stationary surface in contact with a rough, oscillating semi-infinite body (I and II, respectively, in Fig. 1). It is further assumed that the contact asperities have constant square cross-section (2L×2L) and are arranged in a square pattern with a spacing distance S over the free surface of the

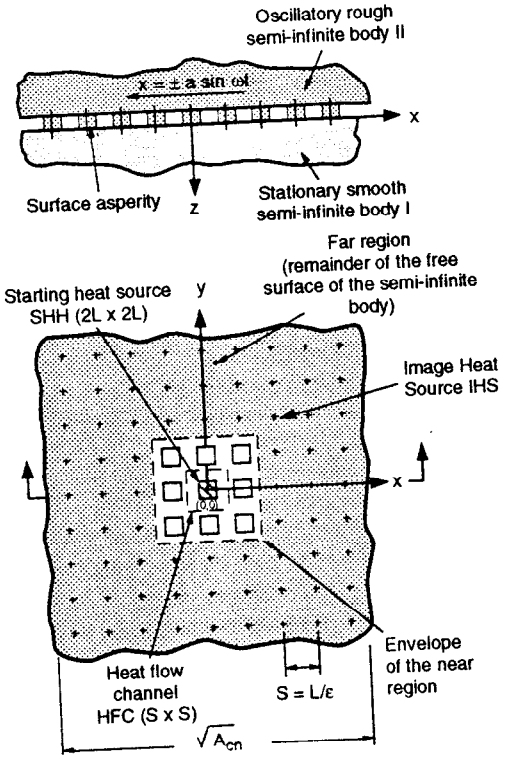

FIG. 1 ARRANGEMENT OF THE STARTING HEAT SOURCE, AND IMAGE HEAT SOURCES IN THE NEAR- AND FAR- REGIONS

half-space I. The analysis is also based on the following assumptions:

i) The relative displacement between the two semi-infinite bodies is described by a simple harmonic motion: $x = a \sin(\omega t)$, where a and ω are the amplitude and the circular frequency of reciprocation, respectively.
ii) The coordinate system is attached to the rough, oscillating body II.
iii) Except for the micro-contacts, the free surface of the semi-infinite bodies I and II are adiabatic.
iv) The mechanical characteristics of the process, as well as the thermo-mechanical properties are constant.

As indicated earlier, the volume which encompasses a single micro-contact and extends to some distance into the solid is defined as the elemental heat flow channel **HFC** [13]. The control surface which separates any two adjacent channels is adiabatic. The characteristic dimension S of the **HFC** is the spacing between two neighbouring micro-contacts and is obtained from the analysis of the corresponding mechanical contact problem:

$$\epsilon^2 = \frac{A_{mic}}{A_{hfc}} = \frac{4L^2}{S^2} = \frac{p_a}{p_m} \qquad (1)$$

where,

ε = the constriction ratio

A_{mic}, A_{hfc} = the micro-contact area and the cross-sectional area of the HFC, respectively

p_a, p_m = the applied contact pressure and the flow pressure of the softer material.

From an analytical viewpoint, the heat generated at the micro-contact area can be regarded as an *oscillating heat source* in relation to body I, and as a *stationary heat source* with respect to body II. For a complete analysis of the thermal constriction problem in fretting, the solutions of both modes of motion are sought. It should be remembered that in either case, the heat flux varies sinusoidally with time.

Formulation of the Problem

Superposition of Image Heat Sources.

The solution for the average temperature θ over an area A_λ at depth z within the heat flow channel **HFC** is based on the method of infinite images developed by Beck [15] and Yovanovich et al. [16,17] for static contact. The average temperature rise $\bar{\theta}$ is the superposition of the contribution of the friction heat generated at the micro-contact attached to this HFC (denoted as the starting heat source SHS) $\bar{\theta}_{shs}$, and due to the contributions from all other neighbouring image heat sources $\bar{\theta}_{ihs}$. The latter can be approximately evaluated by grouping the neighbouring image sources into two

regions; namely, the near- and far- regions. In the *near region*, which surrounds the starting heat source and covers a small portion of the contact interface, only a finite number of frictional heat sources [N_{nr}-1] is considered. In the *far region*, which covers the remainder of the free surface of the semi-infinite body, the friction heat input of the discrete image sources is assumed to be evenly spread. The effective uniform heat flux q_e over the *far region* is described by the following relation:

$$q_e = \epsilon^2 \tilde{q} = \epsilon^2 \mu p_m |V(t)| = \epsilon^2 \mu p_m a \omega |\cos(\omega t)| \quad (2)$$

where, $\tilde{q}$ is the heat flux over the micro-contact area A_{mic}, and μ is the coefficient of friction. The contribution of the *far region* $\bar{\theta}_{fr}$ to the average temperature rise over the area A_λ is the difference between the average temperature rise $\bar{\theta}_{qe,\infty}$ produced by heating the free surface of the semi-infinite body by the effective heat flux q_e and the average temperature drop $\bar{\theta}_{qe,nr}$ due to a negative heat flux ($-q_e$) over the square area of the *near region* bounded by the lines: x,y = $\pm$ [($\sqrt{N_{nr}}$) / 2S]. Therefore, the average temperature rise $\bar{\theta}$ is given by the following relation:

$$\bar{\theta}(x,y,z,t) = \left[\bar{\theta}_{shs}\right] + \left[\sum_{j=1}^{N_{nr}-1} \{\bar{\theta}_{ihs}\}_j\right] + \left[\{\bar{\theta}\}_{qe,\infty} - \{\bar{\theta}\}_{qe,nr}\right] \quad (3)$$

The analysis presented in [1] for N_{nr}= 9 confirmed that this superposition approach satisfies the boundary conditions of the HFC model, in which the control surfaces x,y = $\pm$ S are adiabatic.

In the following section, the solution for the average temperatures $\bar{\theta}_{shs}$, $\bar{\theta}_{ihs}$, $\bar{\theta}_{qe,\infty}$ and $\bar{\theta}_{qe,nr}$ are obtained by integrating the fundamental solution for an instantaneous point source of heat acting on a semi-infinite body with respect to time and the appropriate space variables.

Average Temperatures

To determine the thermal constriction resistance R_c, it is necessary to utilize the average temperatures over the micro-contact area and the HFC cross sectional-area at different planes z $\geq$ 0. The average temperature $\bar{\theta}$ over a square area A_λ = 2λ×2λ, located at (x_a,y_a,z_a) due to an oscillatory, sinusoidal heat source $\tilde{q}$ located at x_s= y_s= z_s = 0. and covers an area 2δ×2δ (Fig. 2) is obtained from the following relation:

$$\bar{\theta}(z,t) = \left[\frac{1}{A_\lambda}\right] \int_{x_a-\lambda}^{x_a+\lambda} \int_{y_a-\lambda}^{y_a+\lambda} \theta(x,y,z,t)\, dx\, dy \quad (4)$$

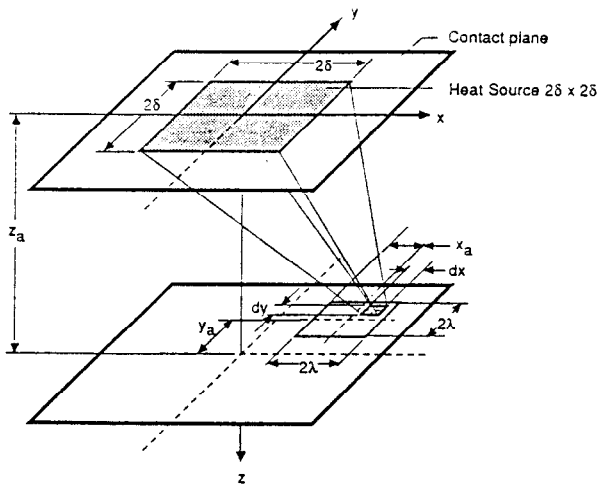

FIG. 2 AVERAGE TEMPERATURE RISE OVER A SQUARE AREA 2λ×2λ AT (x_a,y_a,z_a) DUE TO A FRICTION HEAT SOURCE LOCATED AT O(0,0,0) AND COVERS A SQUARE AREA 2δ × 2δ

The expression for the temperature rise θ(x,y,z,t) at time t and at any point P(x,y,z) within the HFC was obtained in [1]. For the purpose of completeness and clarity, the derivation of this expression and its presentation in dimensionless form are summarized in Appendix A:

$$\Theta(\bar{x},\bar{y},\bar{z},\tilde{t}) = \frac{\sqrt{\pi}}{8} \sqrt{Fo}\; f_p \int_{\Delta\tilde{t}=0} \left([F(\bar{x})]\,[F(\bar{y})] \right) [F(\bar{z})]\, \frac{|\cos 2\pi (\tilde{t}-\Delta\tilde{t})|}{\sqrt{\Delta\tilde{t}}}\, d\Delta\tilde{t} \quad (5)$$

Integration of Eq. 5 with respect to the dimensionless space coordinates $\bar{x}$ and $\bar{y}$ yields the following expression:

$$\bar{\Theta}(\bar{z},\tilde{t}) = \frac{\sqrt{\pi}}{8} \sqrt{Fo}\, [\, f_a\, f_p] \int_{\Delta\tilde{t}=0}^{\Delta\tilde{t}=\tilde{t}} \left([\bar{F}(\bar{x})]\,[\bar{F}(\bar{y})] \right) [\bar{F}(\bar{z})]\, \frac{|\cos 2\pi (\tilde{t}-\Delta\tilde{t})|}{\sqrt{\Delta\tilde{t}}}\, d\Delta\tilde{t} \quad (6)$$

where, $\bar{x}$, $\bar{y}$, and $\bar{z}$= x/L, y/L, and z/L, respectively. The dimensionless temperature $\bar{\Theta}$ is related to the average temperature $\bar{\theta}$ (Eq. 4), the material thermal conductivity k, the contact length L, and the average friction heat input to the system q_{av} by the following relation:

$$\bar{\Theta} = \frac{\bar{\theta}}{q_{av}\, L/k} = \frac{\bar{\theta}\, k}{(\mu\, p_c)\,(a f)\, L} \qquad (7)$$

The other dimensionless parameters in Eq. 6 are defined as:

$$\bar{F}(\bar{z}) = \exp\left(-\frac{\bar{z}^2}{4\,\Delta\tilde{t}\,Fo}\right)$$

$$\bar{F}(\bar{x}) = (2\,\bar{\lambda}) + \sqrt{\Delta\tilde{t}\,Fo}\,[ierfc(A_{\bar{x}}) + ierfc(B_{\bar{x}})] + \sqrt{\Delta\tilde{t}\,Fo}\,[-ierfc(C_{\bar{x}}) - ierfc(D_{\bar{x}})]$$

$$\bar{F}(\bar{y}) = (2\,\bar{\lambda}) + \sqrt{\Delta\tilde{t}\,Fo}\,[ierfc(A_{\bar{y}}) + ierfc(B_{\bar{y}})] + \sqrt{\Delta\tilde{t}\,Fo}\,[-ierfc(C_{\bar{y}}) - ierfc(D_{\bar{y}})]$$

$$A_{\bar{x}} = \frac{\bar{\delta} + (\bar{x}_a + \bar{\lambda}) - \bar{A}\sin(2\pi\tilde{t}) + \bar{A}\sin 2\pi(\tilde{t}-\Delta\tilde{t})}{2\sqrt{[\Delta\tilde{t}\,Fo]}}$$

$$B_{\bar{x}} = \frac{\bar{\delta} - (\bar{x}_a - \bar{\lambda}) + \bar{A}\sin(2\pi\tilde{t}) + \bar{A}\sin 2\pi(\tilde{t}-\Delta\tilde{t})}{2\sqrt{[\Delta\tilde{t}\,Fo]}} \qquad (8)$$

$$C_{\bar{x}} = \frac{\bar{\delta} + (\bar{x}_a - \bar{\lambda}) - \bar{A}\sin(2\pi\tilde{t}) + \bar{A}\sin 2\pi(\tilde{t}-\Delta\tilde{t})}{2\sqrt{[\Delta\tilde{t}\,Fo]}}$$

$$D_{\bar{x}} = \frac{\bar{\delta} - (\bar{x}_a + \bar{\lambda}) + \bar{A}\sin(2\pi\tilde{t}) + \bar{A}\sin 2\pi(\tilde{t}-\Delta\tilde{t})}{2\sqrt{[\Delta\tilde{t}\,Fo]}}$$

$$A_{\bar{y}} = \frac{\bar{\delta} + (\bar{x}_a + \bar{\lambda})}{2\sqrt{[\Delta\tilde{t}\,Fo]}}, \qquad B_{\bar{y}} = \frac{\bar{\delta} - (\bar{x}_a - \bar{\lambda})}{2\sqrt{[\Delta\tilde{t}\,Fo]}}$$

$$C_{\bar{y}} = \frac{\bar{\delta} + (\bar{x}_a - \bar{\lambda})}{2\sqrt{[\Delta\tilde{t}\,Fo]}}, \qquad D_{\bar{y}} = \frac{\bar{\delta} - (\bar{x}_a + \bar{\lambda})}{2\sqrt{[\Delta\tilde{t}\,Fo]}}$$

$$\bar{t} = \frac{\alpha\, t}{L^2},\quad \tilde{t} = \frac{\alpha\, t}{L^2},\quad \tilde{t} = \frac{t}{\tau} = \frac{\bar{t}}{Fo},\quad \Delta\tilde{t} = \tilde{t} - \bar{t},\quad Fo = \frac{\alpha}{f L^2}$$

The symbols $\bar{\delta}$ and $\bar{\lambda}$ are the dimensionless characteristics length of the heat source, $\bar{\delta} = \delta/L$, and the area A_λ over which the temperature is averaged, $\bar{\lambda} = \lambda/L$. The factor f_a in Eq. 6 is the ratio between the area of the starting heat source A_{mic} and the area A_λ; $f_a = 1/\bar{\lambda}^2$. The factor f_p is the ratio between the contact pressure p_c over the area of the friction heat source and the flow pressure of the softer material; $f_p = p_c / p_m$.

In the special case when the heat source is *stationary*, i.e., attached to the body, but is still varying sinusoidally with time, the average temperature at any depth $\bar{z}$ can be obtained from Eq. 6 after substituting for the dimensionless oscillation amplitude $\bar{A} = 0$ in the functions $A_{\bar{x}}$, $B_{\bar{x}}$, $C_{\bar{x}}$ and $D_{\bar{x}}$ in Eq.8. Equation 6 provides also the solution for the average temperatures in *static contact* when the strength of the heat source is time-independent and has the same average of the sinusoidal frictional heat. In such a case, the quantity $|\cos(2\pi(\tilde{t}-\Delta\tilde{t}))|$ is replaced by $(2/\pi)$ and the oscillation amplitude $\bar{A} = 0$. As $\bar{\delta}\to\infty$, the average temperature $\bar{\Theta}$ over an area A_λ due to an infinite far-region heat source is determined from the following relation:

$$[\bar{\theta}(\bar{z},\tilde{t})]_{\bar{\delta}\to\infty} = \frac{\sqrt{\pi}}{2}\sqrt{Fo}\; f_a\, f_p \int_{\Delta\tilde{t}=0}^{\Delta\tilde{t}=\tilde{t}} [\bar{F}(\bar{z})]\,\frac{|\cos 2\pi(\tilde{t}-\Delta\tilde{t})|}{\sqrt{\Delta\tilde{t}}}\, d\Delta\tilde{t} \qquad (9)$$

Table 1 shows the dependence of the variables f_a, f_p and $\bar{\delta}$ on the type of heat source and the area A_λ over which the temperature is averaged. The symbol N_{nr} stands for the number of discrete image heat sources in the near region.

TABLE 1. THE PARAMETERS f_a, f_p, AND $\bar{\delta}$ FOR VARIOUS TYPES OF HEAT SOURCES

Heat source → and Averaged area A_λ ↓	starting heat source SHS and image heat source IHS	near region (nr)	far region (fr)
micro-contact area	$f_p=1$, $f_a=1$, $\bar{\delta}=1$	$f_p=\varepsilon^2$, $f_a=1$, $2\bar{\delta}=\sqrt{N_{nr}}/\varepsilon$	$f_p=\varepsilon^2$, $f_a=1$, $\bar{\delta}=\infty$
cross-sec. area of HFC	$f_p=1$, $f_a=\varepsilon^2$, $\bar{\delta}=1$	$f_p=\varepsilon^2$, $f_a=\varepsilon^2$, $2\bar{\delta}=(\sqrt{N_{nr}})/\varepsilon$	$f_p=\varepsilon^2$, $f_a=1$, $\bar{\delta}=\infty$

Thermal Constriction Resistance.

The constriction resistance R_c arises due to the fact that the micro-contact area is smaller than the cross section of the HFC. Frictional heat flow lines Q must, therefore, spread out into the HFC rather than taking the least resistance, straight path. The temperature difference between the average temperature on the micro-contact area $\bar{\Theta}_c$ and the mean temperature $\bar{\Theta}_{m,\bar{z}}$ over the cross sectional area A_{hfc} of the HFC at any plane $\bar{z}$ is due to the total thermal resistance R_t, which includes the resistance R_m of the material of the HFC itself as well as the constriction resistance R_c due to the micro-contact area [13]:

$$Q\,R_c = \left(\frac{1}{A_{mic}}\oint_{A_{mic}} \theta(x,y,0)\,dA_{mic}\right) - \left(\frac{1}{A_{hfc}}\oint_{A_{hfc}} \theta(x,y,z)\,dA_{hfc}\right) - \left(\frac{z}{kA_{hfc}}\right)Q \quad (10)$$

With the assumption that these two resistances are additives, Yovanovich et al. demonstrated [19,20] that the temperature drop due to the constriction resistance only is the difference between the average temperature of the contact area $\bar{\Theta}_c$ and the mean temperature $\bar{\Theta}_{m,\bar{z}=0}$ of the entire contact plane (i.e., the HFC cross-section at $\bar{z}=0$), when the heat source is stationary and time-independent. This conclusion will be tested in the present study, for the case in which the heat source varies sinusoidally, both in the time and space domains.

Due to the cyclic nature of the thermal load, both the instantaneous and average values of the thermal constriction resistance are determined. The instantaneous microscopic thermal constriction resistance $R_{c,inst}$ can be defined in terms of the instantaneous heat flux q_{inst} over the micro-contact area (2Lx2L):

$$R_{c,inst} = \frac{(\bar{\theta}_c - \bar{\theta}_m)_{z=0}}{q_{inst}\,(4L^2)} = \frac{(\bar{\theta}_c - \bar{\theta}_m)_{\bar{z}=0}}{2\pi kL\,|\cos(2\pi\,\tilde{t})|} \quad (11)$$

The dimensionless instantaneous constriction resistance parameter ψ is related to the thermal constriction resistance $R_{c,inst}$ by the following relation [13]:

$$R_{c,inst} = \frac{\psi}{2k\sqrt{A_c}} = \frac{\psi}{4kL} \quad (12)$$

From Eqs. 11 and 12, the following expression for the constriction resistance parameter ψ is obtained:

$$\psi = \left[\frac{2}{\pi}\right]\frac{\left[\bar{\theta}_c - \bar{\theta}_{m,\bar{z}=0}\right]}{|\cos(2\pi\,\tilde{t})|} \quad (13)$$

From Eqs. 6 and 13, one can conclude that the functional relationship between the constriction resistance parameter and Fourier modulus can be described as:

$$\psi = fn\left\{\sqrt{Fo},\ ierfc\left(\frac{f_{\bar{x},\bar{y},\tilde{t},\Delta\tilde{t}}}{\sqrt{Fo}}\right)\right\} \quad (14)$$

where, $f_{\bar{x},\bar{y},\tilde{t},\Delta\tilde{t}}$ is a function of the coordinates $\bar{x}$ and $\bar{y}$, and the time parameters $\tilde{t}$ and $\Delta\tilde{t}$. Therefore, it is predicted that for small values of Fourier modulus Fo, the **ierfc(...)** term dominates and, therefore, the rate of change in the thermal constriction resistance decreases with the increase in Fo. As Fourier modulus increases further, the **ierfc(...)** function approaches zero and ψ becomes a function of $\sqrt{Fo}$ only.

Numerical Solution- Function Behaviour and Singularity.

The integration expressed by Eq. 6, was performed numerically, since no closed-form analytical solution exists. At the lower limit of integration $\Delta\tilde{t} = 0$, the integrand I exhibits a singularity. This singularity was removed by splitting the integral into a singular part $I_s(0 \le \Delta\tilde{t} \le \sigma)$ which is to be treated separately, and a non-singular part $I_{ns}(\sigma < \Delta\tilde{t} \le \tilde{t})$ to which one of the conventional numerical integration methods is applied:

$$\int_{\Delta\tilde{t}=0}^{\Delta\tilde{t}=\tilde{t}} I(...)\,d\Delta\tilde{t} = \int_{\Delta\tilde{t}=0}^{\Delta\tilde{t}=\sigma} I_s(...)\,d\Delta\tilde{t} + \int_{\Delta\tilde{t}=\sigma}^{\Delta\tilde{t}=\tilde{t}} I_{ns}(....)\,d\Delta\tilde{t} \quad (15)$$

To treat the functions $\bar{F}(\bar{x})$ and $\bar{F}(\bar{y})$ in the integrand I_s as constants, i.e., independent of $\bar{x}$ and $\bar{y}$, the initial time step σ is chosen to be sufficiently small to cause the arguments **arg** of the integral complementary error function **ierfc(arg)** to be equal to zero, or to be ≥ 5. In such a case, **ierfc(arg = 0)** = $1/\sqrt{\pi}$, and **ierfc(arg$\ge$5)** can be assumed to be zero, with an error $< 2\times10^{-11}$. For the working range $250 \le FO \le 10^5$, the value of σ is chosen to be equal to 0.5×10^{-8}. Therefore, for $0 \le \Delta\tilde{t} \le \sigma$, the integration of the first term in Eq. 6 can be written as:

$$\bar{\theta}_o(\bar{z},\tilde{t}) = \frac{\sqrt{\pi}}{8}\sqrt{Fo}\ f_s\ f_p\ [C_{\bar{x},\bar{y}}]\ |\cos(2\pi\,\tilde{t})| \int_{\Delta\tilde{t}=0}^{\tilde{t}=\sigma} \exp\left(-\frac{\bar{z}^2}{4\,\Delta\tilde{t}\,Fo}\right)\frac{d\,\Delta\tilde{t}}{\sqrt{\Delta\tilde{t}}} \quad (16)$$

where, $[C_{\bar{x},\bar{y}}] = F_o(\bar{x})\,F_o(\bar{y})$. In what follows, the results of the integration expressed by Eq. 16 is summarized for various types of heat sources. The notation used to express the initial average temperature is $\bar{\Theta}_{o,a,s,d}$. The parameters of the subscript indicate the following: o ≡ this expression is related the temperature rise during the initial time step $\sigma < \tilde{t} < 0$, a ≡ the area that is being averaged (c and m for the contact area and the cross-sectional area of the HFC, respectively), s ≡ the type of heat source (shs, ihs, nr or fr), and d ≡ the depth of the area being average ($\bar{z}=0$ or $\bar{z} > 0$).

i- Starting heat source SHS; $\bar{x}_a=\bar{y}_a=0$ and $\bar{\delta}=1$:

a) average temperature $\bar{\Theta}_{c,o}$ over the micro-contact area; $\lambda=1$ and $\bar{z}=0$:

In this case, $\bar{F}_o(\bar{x}) = \bar{F}_o(\bar{y}) = [\,2 - 2\sqrt{(Fo/\pi)}\sqrt{(\Delta\tilde{t})}\,]$, and

$$\bar{\theta}_{o,c,shs,\bar{z}\geq 0} = B_1 \left|\cos(2\pi\tilde{t})\right| \int_0^{\sigma} \frac{1}{\Delta\tilde{t}}\left[4 - 8\sqrt{\frac{Fo}{\pi}}\sqrt{\Delta\tilde{t}} + \frac{4Fo}{\pi}\Delta\tilde{t}\right] d\Delta\tilde{t} \quad (17)$$

where, $B_1 = ([\sqrt{\pi}]/[8\sqrt{Fo}])\, f_a\, f_p$. The values of f_a and f_p are given in Table 1. For the special case when $\bar{z} = 0$, the integration of Eq. 17 results in the following expression:

$$\bar{\theta}_{o,c,shs,\bar{z}=0} = B_1 \left|\cos(2\pi\tilde{t})\right| \left[8\sqrt{\sigma} - 8\sqrt{\frac{Fo}{\pi}}\sigma + \frac{8\,Fo}{3\pi}\sigma^{3/2}\right] \quad (18)$$

b) average temperature $\bar{\Theta}_{o,m,shs,\bar{z}\geq 0}$ over the cross-sectional area of the HFC; $\bar{\lambda}=1/\varepsilon$ and $\bar{z} \geq 0$:

In this case, the functions $\bar{F}(\bar{x}) = \bar{F}(\bar{y}) = 2$, and

$$\bar{\theta}_{o,m,shs,\bar{z}>0} = 4 B_1 \left|\cos(2\pi\tilde{t})\right| \int_0^{\sigma} \frac{\exp\left(\frac{-C_n}{2\Delta\tilde{t}}\right)}{\Delta\tilde{t}} d\Delta\tilde{t} \quad (19)$$

Through successive integration by parts, the solution of Eq. 19 is obtained:

$$\bar{\theta}_{o,m,shs,\bar{z}>0} = 8 B_1 \left|\cos(2\pi\tilde{t})\right| \sqrt{C_n} \left[\exp\left(-\frac{C_n}{2\sigma}\right) S_{n1}\right] + 2\sqrt{C_n}\, R_{n1} \quad (20)$$

where the asymptotic series S_{n1} is defined by the following equation:

$$S_{n1} = \sum_{n=1} \frac{(-1)^{n-1}\, 1.3.5 \ldots (2n-1)}{[C_n/\sigma]^{\left(\frac{2n+1}{2}\right)}} \quad (21)$$

where, $C_n = \bar{z}/[2\,Fo]$. Examination of the series S_{n1} indicated that the number of terms N used in the computation should be ≤7, to ensure its convergence for all values of $C_n \geq 15$. The truncation error R_{n1} involved in omitting other terms N >7 is:

$$|R_{n_1}| \leq \frac{1.3.5 \ldots (2n+1)}{[C_n/\sigma]^{\left(\frac{2n+3}{2}\right)}} \exp\left(-\frac{C_n}{2\sigma}\right) \leq 2\times 10^{-6} \quad (22)$$

In the special case when $\bar{z}=0$, the value of $\bar{\Theta}_{o,m,shs,\bar{z}=0}$ is described by the following relation:

$$\bar{\theta}_{0,m,shs,\bar{z}=0} = 8 B_1 \left|\cos(2\pi\tilde{t})\right| \sqrt{\sigma} \quad (23)$$

ii- Image heat sources in the near region IHS; $\bar{x}_a \neq 0$, or $\bar{y}_a \neq 0$, and $\bar{\delta}= 1$:

In this case, the functions $\bar{F}(\bar{x}) = \bar{F}(\bar{y}) = 0$. The average temperature over the micro-contact area and the cross-sectional area of the HFC for all values of $\bar{z} \geq 0$ are therefore: $\bar{\Theta}_{o,c,ihs,\bar{z}\geq 0} = \bar{\Theta}_{o,m,ihs,\bar{z}\geq 0} = 0$.

iii- Near region heat source; $\bar{x}_a = \bar{y}_a = 0$, $\bar{\delta} = N_l/\varepsilon$:

The average temperature $\bar{\Theta}_{o,c,nr,\bar{z}=0}$ over the micro-contact area, where $\bar{\lambda}=1$, and $\bar{z} = 0$, is similar to the solution obtained for the SHS and given by Eqs. 17 and 18. Over the cross-sectional area of the HFC, where $\bar{\lambda}=1/\varepsilon$ and $\bar{z} \geq 0$, the functions $\bar{F}(\bar{x}) = \bar{F}(\bar{y}) = 2/\varepsilon$, and therefore, the solutions for the average temperature $\bar{\Theta}_{o,m,nr,\bar{z}\geq 0}$ is similar to those given by Eqs. 19 and 20, using the appropriate value of f_a, as per Table 1, and after replacing B_1 by B_1/ε^2.

iv- Far region heat source; $\bar{x}_a = \bar{y}_a = 0$, and $\bar{\delta} = \infty$:

The average temperature $\bar{\Theta}_{o,c,fr,\bar{z}=0}$ over the micro-contact area, or the average temperature rise $\bar{\Theta}_{o,m,fr,\bar{z}\geq 0}$ over the cross-sectional area of the HFC at $\bar{z} \geq 0$, are also similar to the solution obtained for the SHS and given by Eqs. 18 and 20, after substituting for the factor $f_a = 1$ in the coefficient B_1.

To ensure that the non-singular part I_{ns} of the integrand in Eq. 6 is accurately represented by a quadrature formula of n=2, the behaviour of the integrand was examined over a number of cycles $n < 5$. Figure 3 shows the steep drop in the integrand I_{ns} within $\sigma = 0.5\times 10^{-8} < \tilde{t} < 0.0025$. This peculiar behaviour may lead to a significant error in estimating the average temperatures and the constriction resistance, unless the number of divisions for numerical integration is sufficiently large. In validating the formulation and numerical treatment presented in this paper, Eq. 6 was used to calculate the static thermal constriction parameter ψ_s and was compared with Yovanovich's correlation [19]:

$$\psi_s = c_1 (1-\varepsilon)^{c2}, \quad \text{where } \varepsilon \leq 0.3 \quad (24)$$

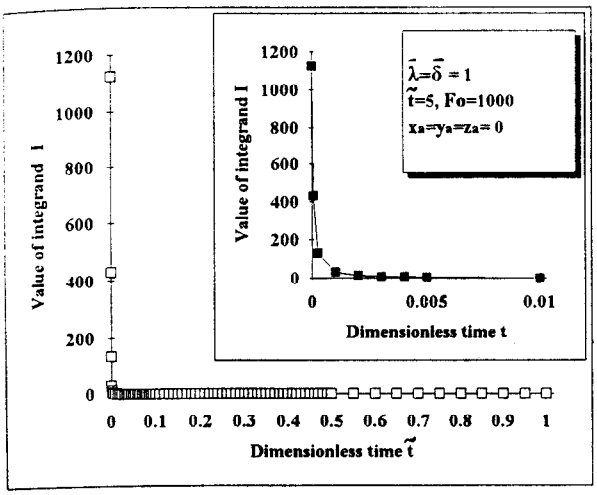

FIG. 3 BEHAVIOUR OF THE INTEGRAND I_{ns} IN EQ. 6 DURING THE FIRST CYCLE (Fo=10^3, $\bar{A}=\bar{\lambda}=\bar{\delta}=1$, $\bar{x}_a=\bar{y}a=\bar{z}=0$, $\tilde{t}=5$)

For a square contact area, the coefficients c_1 and c_2 in Eq. 24 are 0.958 and 1.35, respectively. It has been found that the relative error between Eq. 24 [19] and Eq. 6 in the present analysis is <1.5%, when the number of divisions N_{intg} for numerical integration are: $N_{intg} \geq 1500$ for $0.5\times10^{-8} < \tilde{t} < 0.001$, $N_{intg} \geq 800$, for $0.001 < \tilde{t} < 0.01$, $N_{intg} \geq 500$ for $0.01 < \tilde{t} < 1$, and $N_{intg} \geq 10$ for $\tilde{t} > 1$. These number of divisions were used in generating the results presented in the next section.

RESULTS AND DISCUSSION

The effects of the following process variables on the thermal constriction parameter ψ are examined: Fourier modulus: $250 \leq Fo \leq 10^5$, the amplitude ratio $0.5 \leq \bar{A} \leq 10$, and the constriction ratio $\varepsilon \leq 0.25$. These ranges cover the typical fretting conditions encountered in most practical applications: frequency: $2.5 \leq f \leq 100$ Hz, slip amplitude: $5 \leq a \leq 100$ μm, and thermal diffusivity: $5 \leq \alpha \leq 80$ mm^2 s^{-1}.

Characteristic Features of the Constriction Parameter ψ, during the Quasi-Steady State Cycle:

For all combinations of process variables that have been tested in this work, the quasi-steady state cycle was reached after 5 to 10 cycles only. The analysis carried out by Attia and Camacho [1] showed that the steady cyclic variation in the temperature field was reached after 2×10^3 cycles, when $\bar{A}$ = 10, ε = 0.2, Fo = 10^3, and the ratio γ of the contour area (far region heat source) to the micro-contact area = 100. This supports the observations made in [15,16] that although no steady state condition exists for the temperature field in the presence of an infinite number of micro-contacts, the difference between the average contact temperature $\bar{\Theta}_c$ and the average temperature $\bar{\Theta}_m$ of the HFC cross-section at some plane $\bar{z}$ converges rapidly to the steady state.

Figure 4 shows the change in the constriction parameter ψ during the quasi-steady state cycle $\tilde{t}$, for different values of Fourier modulus, $250 \leq Fo \leq 10^5$. The ends of the oscillation stroke, $\tilde{t}$=0.25 and 0.75, present singularity points since the relative velocity between the contacting solids and consequently the frictional heat generation reach zero. Therefore, the constriction resistance and the parameter ψ approach infinity. Fortunately, this singularity in the system behaviour has no practical significance, since the exercise of heat partitioning is meaningless when the instantaneous level of frictional heat is zero in the first place. Figure 4 indicates also that for Fo> 10^3, the variation in the parameter ψ with time is insignificant. Apart from the singularity points at $\tilde{t}$ = (0.25 and 0.75) ± 0.05, the constriction parameter ψ varies only within ± 4.5 % of its average value, in the worst case when Fo = 250. For all practical purposes, the constriction parameter is assumed to be time-independent, and only its average value $\bar{\psi}$ is to be considered. The results presented in [1] showed that while there is a significant time lag for the maximum temperature rise at different points within the HFC, $\bar{z} \leq 10$, the phase difference between the average temperature $\bar{\Theta}_c$ of the micro-contact area and the mean temperature $\bar{\Theta}_m$ of the contact plane, i.e., the cross sectional area of the HFC at $\bar{z}$ = 0, is ≤ 3°. This in agreement with the results shown in Fig. 4, which shows that phase difference $\Delta\phi$ between the frictional-heat source and the thermal constriction parameter ψ is nearly zero.

Figure 5 shows that the temperature difference $\Delta\bar{\Theta} = (\bar{\Theta}_c - \bar{\Theta}_{m,\bar{z}\geq0})$ between the average temperatures of the micro-contact area and the mean temperature of the cross-sectional area of the HFC at $\bar{z} \geq 0$ varies linearly with depth $\bar{z}$. This indicates that the two components of the total resistance R_t; namely the constriction resistance R_c and the resistance of

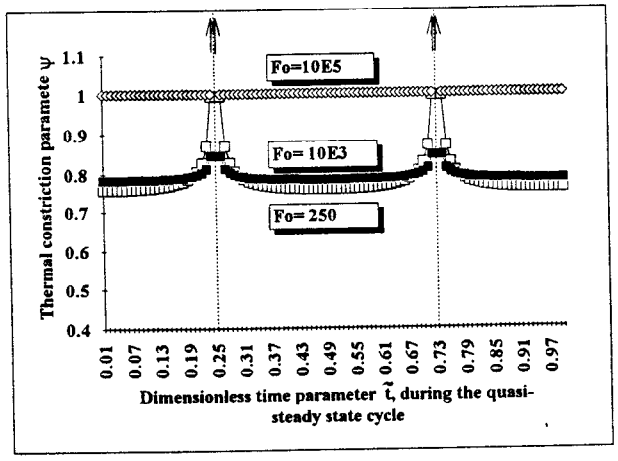

FIG. 4 VARIATION OF THE CONSTRICTION PARAMETER DURING THE QUASI-STEADY STATE CYCLE (ε = 0.15, $\bar{A}$=10, OSCILLATION, AND Fo = 250, 10^3, 10^5)

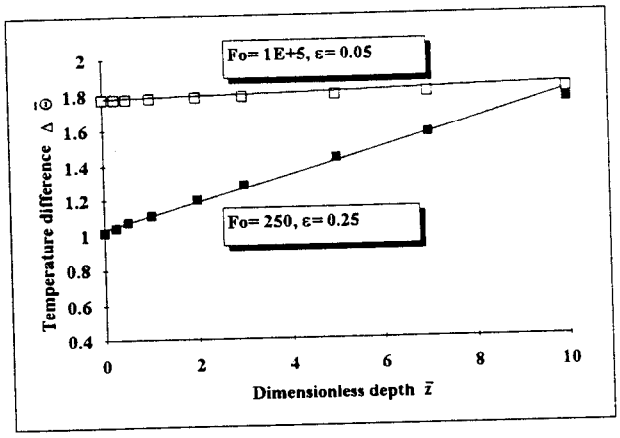

FIG. 5 DISTRIBUTION OF THE TEMPERATURE DIFFERENCE ($\Delta\bar{\Theta} = \bar{\Theta}_c - \bar{\Theta}_m$) ALONG THE DEPTH $\bar{z}$

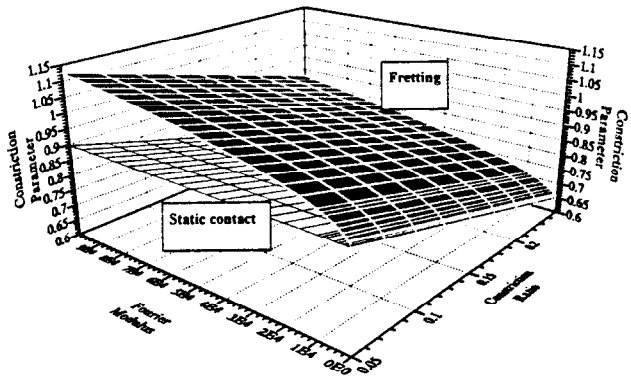

FIG. 6 EFFECT OF FOURIER MODULUS Fo, AND THE CONSTRICTION RATIO ε ON THE AVERAGE CONSTRICTION PARAMETER $\bar{\psi}$ IN FRETTING AND IN STATIC CONTACT

the material of the HFC itself $\mathbf{R_m}$, are indeed additive. This conclusion is in agreement with the theory of constriction resistance in static contact [15-17]. The graph indicates also that the extrapolation of the difference in the average temperatures $(\bar{\Theta}_c - \bar{\Theta}_{m,\bar{z}>0})$ to the contact plane, $\bar{z}=0$, coincides with the direct calculation of $(\bar{\Theta}_c - \bar{\Theta}_{m,\bar{z}=0})$. Therefore, in determining the average constriction resistance parameter $\bar{\psi}$, only the quantity $(\bar{\Theta}_c - \bar{\Theta}_{m,\bar{z}=0})$ needs to be calculated.

Effect of Process Parameters on the Average Constriction Parameter $\bar{\psi}$

Effect of Fourier Modulus Fo, and the Constriction Ratio ε

Figure 6 shows the dependence of the average constriction parameter $\bar{\psi}$ on the constriction ratio, $0.05 \le \varepsilon \le 0.25$, and fourier modulus, $250 \le Fo \le 1\times10^5$. The figure includes also the relationship between $\bar{\psi}_s$ and ε for static contact, i.e., when the heat source is stationary and time-independent (Eq. 24 [19]). The following observations can be made. First, the increase in the constriction ratio ε results in a nearly linear reduction in the constriction resistance. This negative effect is expected, since at the limit when $\varepsilon \to 1$, the constriction (or spreading-out) phenomenon will no longer exist, and the constriction resistance approaches zero. Second, the increase in Fourier modulus, $Fo=\alpha/(fL^2)$, leads to an increase in the constriction parameter $\bar{\psi}$. It is also worth noting that the rate of change $\partial\bar{\psi}/\partial Fo$ is more significant at lower levels of Fourier modulus, $Fo \le 10^4$, as suggested by Eq. 14. On some physical grounds, one can argue that at high frequencies of oscillation (small Fourier modulus), the front of the thermal wave is very close to the contact area causing the *effective* constriction ratio to be close to unity, and constriction parameter $\bar{\psi}$ to approach 0. As the penetration depth increases (proportional to $\sqrt{Fo}$), the skin effect becomes less pronounced and the *effective* constriction ratio becomes smaller. This leads to the increase in the constriction parameter. With a further increase in Fourier modulus, the front of the thermal wave reaches the adiabatic control surfaces containing the **HFC**, leading to a reduction in the rate of change in the thermal constriction resistance. This reasoning, which explains the trend of the results given in Fig. 6, is consistent with the results reported by Yovanovich et al. [20-22] for the transient constriction resistance for a single and multiple contacts on a half-space.

Comparison of the constriction parameter results $\bar{\psi}$ obtained in this study with the static constriction resistance parameter ψ_s (Eq. 24) indicates that $\bar{\psi} > \psi_s$ for $250 \le Fo \le 10^5$, and $\varepsilon \le 0.25$. In fact, the surface representing the $\bar{\psi}\{\varepsilon,Fo\}$ relationship intersects with the $\psi_s\{\varepsilon\}$ plane at Fo=250. Some tests were conducted for $Fo < 250$, and the results showed that in this range the behaviour is reversed: $\bar{\psi}<\psi_s$. For example, when $\varepsilon = 0.15$, $\psi_s = 0.769$, while $\bar{\psi} = 0.661$, 0.729, 0.762, and 0.768, for Fo= 50, 100, 200, and 250, respectively.

Effect of the mode of motion

As indicated earlier, the contacting solids can be regarded as moving (oscillatory in this case) and stationary bodies in relation to the frictional heat source. These two modes of motion are denoted as mode I and II, respectively. The ratio between the constriction resistance parameter in mode II to that in mode I, $R_{\bar{\psi}} = \bar{\psi}_{II}/\bar{\psi}_I$, is presented in Fig. 7, for $0.05<\varepsilon<0.25$, and $250<Fo<5\times10^3$. Figure.7 shows that the $R_{\bar{\psi}} < 1.03$ and is very small for $Fo > 5\times10^3$ (less than 1.001). Therefore, one can conclude that the mode of motion has insignificant effect on the constriction resistance $\mathbf{R_c}$ (<3%), and that the increase in $\mathbf{R_c}$ (as compared with the case of static contact, Fig. 6) is due to the sinusoidal variation of the frictional heat with time, rather than the harmonic motion.

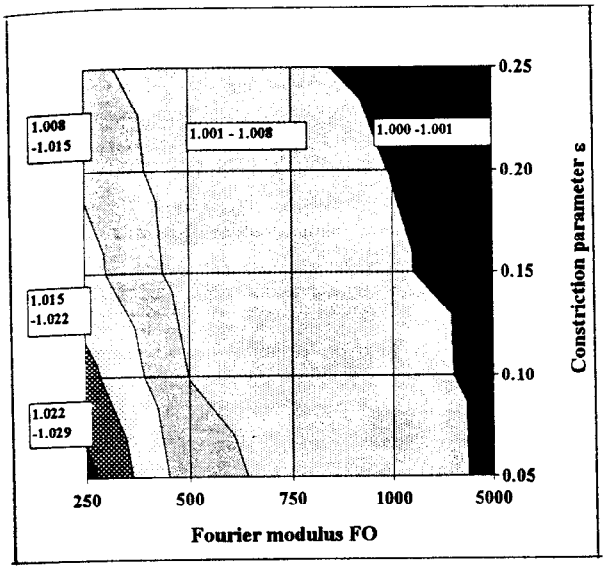

FIG. 7 EFFECT OF FOURIER MODULUS Fo, AND THE CONSTRICTION RATIO ε ON THE RATIO $R_{\bar{\psi}}$

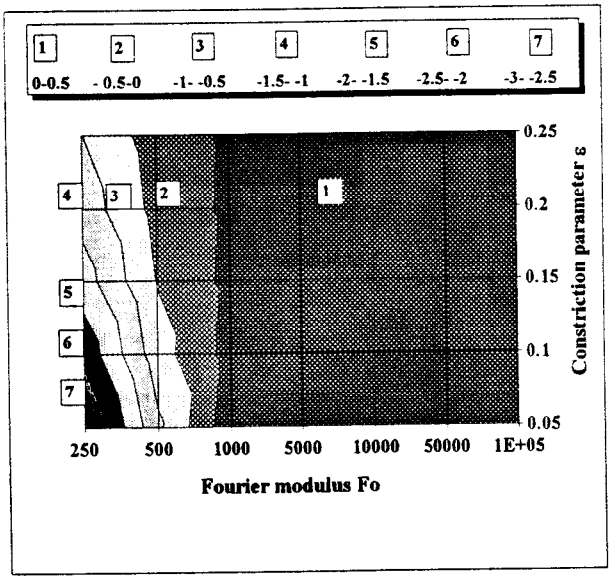

FIG. 8 THE RELATIVE ERROR IN ESTIMATING THE CONSTRICTION PARAMETER $\bar{\psi}$ FOR $0.5<\bar{A}<10$, WITH RESPECT TO THE REFERENCE CASE $\bar{A}=10$

Effect of the Amplitude of Motion $\bar{A}$

The effect of increasing the amplitude of motion from $\bar{A}$ = 0.5 to $\bar{A}$ = 10 on the $\bar{\psi}\{\varepsilon,Fo\}$ relationship has been examined. Considering the case in which $\bar{A}$ = 10 as a reference case, the relative deviation in the average constriction resistance parameter as $\bar{A}$ is changed to $\bar{A}$ = 0.5 is presented in Fig. 8. The figure shows that a twenty-fold change in the amplitude of motion results in < 3% change in predicted value of the constriction parameter $\bar{\psi}$.

THE CORRELATION BETWEEN THE AVERAGE CONSTRICTION PARAMETER $\bar{\psi}$ AND THE PROCESS VARIABLES

Since the mode and the amplitude of motion have insignificant effect on the average constriction parameter, only the effects of Fourier modulus and the constriction ratio need to be considered. A non-linear least square iterative procedure was used to curve fit the surface $\bar{\psi}\{\varepsilon,Fo\}$ shown in Fig. 6. The S-shaped surface suggested a mathematical relation of the following form:

$$\bar{\psi} = \dot{A} + \dot{B}\sinh[\dot{C}\log(Fo)] + \dot{D}\,\epsilon \qquad (25)$$

The constants were found to be: A`= 0.948, B`= 0.0017, C`=0.489, and D`= -1.256. If the constant C` is taken to be 0.5, then Eq. 25 can further be simplified to the following mathematical form:

$$\bar{\psi} = A + B\sqrt{Fo} + \frac{C}{\sqrt{Fo}} + D\,\epsilon \qquad (26)$$

The constants in Eq. 26 were found to be: A= 0.953, B= 0.00074, C= 0.0955, and D= -1.256. Eq. 26 suggests that while the constriction resistance depends on √Fo, there are two interacting and opposite mechanisms the govern this relation. As mentioned earlier, this is physically related to the effect of Fo on the extent of the thermally disturbed zone in relation to the whether or not the front of the thermal wave reaches the adiabatic control surfaces of the HFC.

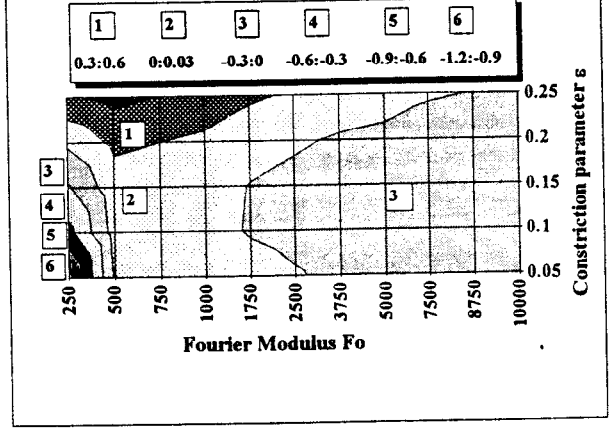

Fig. 9 A MAP FOR THE RELATIVE ERROR IN DETERMINING THE CONSTRICTION PARAMETER $\bar{\psi}$, USING EQ. 26

Figure 9 shows the relative error in estimating $\bar{\psi}\{\varepsilon,Fo\}$ using Eq. 26. The maximum relative error is found to be < 1.25%. For $Fo>10^4$, the relative error is <0.3%. This range is, therefore, omitted from the graph. For any given operating conditions, the maps given in Figs. 7 to 9 provide an estimate of the approximation associated with Eq. 26.

CONCLUSIONS

The following conclusions can be drawn from the present study:

1- A general model has been developed to determine the thermal constriction resistance $\mathbf{R_c}$ of the stationary and oscillating bodies in contact during fretting. The model is capable of predicting $\mathbf{R_c}$ in the transient and quasi-steady states.

2- For the working range covered in this study: $250 < Fo < 10^5$, $\varepsilon < 0.25$, and $0.5 < \bar{A} < 10$, the thermal constriction resistance in fretting $\mathbf{R_c}$ is greater than that in static contact $\mathbf{R_{c,s}}$. This effect is more pronounced at higher levels of Fourier modulus Fo (at $\varepsilon = 0.25$, the ratio $\mathbf{R_c/R_{c,s}} = 1$ and 1.36 at $Fo = 250$ and 10^5, respectively).

3- For the working range considered in this study, the thermal constriction resistance $\mathbf{R_c}$ is nearly constant (variation around the mean value is $< \pm 5\%$) during the quasi-steady state. The constriction resistance $\mathbf{R_c}$ is also nearly independent of the amplitude of oscillation and mode of motion (with variation < 3 %).

4- The correlation between the constriction parameter $\bar{\psi}$ and the process parameters Fo and ε has been established. Error maps to estimate the effect of neglecting the effects of the amplitude of oscillation and mode of motion are provided.

ACKNOWLEDGMENT

The authors wishes to acknowledge the partial financial support of the Natural Sciences and Engineering Research Council of Canada NSERC. The authors also thank Dr. F. Camacho, of Ontario Hydro Technologies for his assistance and guidance in performing the curve fitting of the results.

REFERENCES

1- Attia, M.H., and Camacho, F., "Temperature Field in the Vicinity of a Contact Asperity during Fretting", Proceedings of the ASME Symposium on Contact Problems and Surface Interactions in Manufacturing and Tribological Systems, edited by M.H. Attia and R. Komanduri. ASME Winter Annual Meeting, New Orleans, Louisiana, December 1993.

2- Waterhouse, R.B., "Fretting at High Temperature", Tribology International, vol. 14, 1981, pp. 203-209.

3- Bill, R.C., "The Role of Oxidation in the Fretting Wear Process", Proc. Int. Conf. on Wear of Materials, San Francisco, CA., 1981, American Society of Mechanical Engineers, N.Y., pp. 238-250.

4- Hurricks, P.L., and Ashford, K.S., "The Effect of Temperature on the Fretting Wear of Mild Steel", J. Inst. Mech. Engrg., London, 184(3L), 1969-1970.

5- Kayaba, T., and Iwabuchi, A., "The Fretting wear of 0.45% Carbon steel and Austenitic Stainless steel from 20°C up to 650°C in air", Proc. Int. Conf. on Wear of Materials, San Francisco, Ca., 1981, American Society of Mechanical Engineers, N.Y., pp. 229-237.

6- Attia, M.H., "Friction-Induced Thermoelastic Effects due to Fretting Action", presented at and submitted for publication in the Proceedings of the ESIS International Conference on Fretting Fatigue, Sheffield, U.K., April 1993.

7- Attia, M.H., and D'Silva, N.S., "Effect of Mode of Motion and Process Parameters on the Prediction of Temperature Rise in Fretting Wear", Wear, Vol. 106, 1985, pp.203-224.

8- Attia, M.H., "Friction-Induced Temperature Rise in Fretting- Elemental Heat Flow channel Model", Proc. International congress on tribology, ed. by K. Holmberg and I. Nieminen, Helsinki, Finland, 1989, vol. 3, pp. 22-29.

9- Ling, F.F., and Pu, S.L., "Probable Interface Temperatures of Solids in Sliding Contact", Wear, vol. 7, 1964, pp.23-34.

10- Day, A.J., "An Analysis of Speed, Temperature, and Performance Characteristics of Automotive Drum Brakes", Trans. ASME, J. Tribology, vol. 110, April 1988, pp. 298-305.

11- Berry, G.A., and Barber, J.R., "The Division of Frictional Heat- A Guide to the Nature of Sliding Contact", Trans. ASME, J. Tribology, vol. 106, July 1984, pp. 405-415.

12- Floquet, A., and Play, D., "Contact Temperature in Dry Bearings. Three Dimensional Theory and Verification", Trans. ASME, J. Lubrication Technology, April, 1981, vol. 103, pp.243-252.

13- Yovanovich, M.M., "Thermal Contact Resistance: Theory and Applications", Lecture Notes, Mechanical Engineering Department, University of Waterloo, Canada, 1976.

14- Tsukada, T. and Anno, Y., "Analysis of the Deformation of Contacting Rough Surfaces", Bull. JSME, vol. 15, No. 86, 1972, pp. 996-1003

15- Beck, J.V., "Effect of Multiple Sources in the Contact Conductance Theory", ASME Trans., J. of Heat Transfer, vol. 101, Feb. 1979, pp. 132-136.

16- Negus, K.J., Yovanovich, M.M., and DeVaal, J.W., "Development of Thermal Constriction Resistance for Anisotropic Rough Surfaces by the Methods of Infinite Images", National Heat Transfer Conf., Denver, Co. August 1985, ASME, N.Y.

17- Negus, K.J., and Yovanovich, M.M., "Application of the Method of Optimized Images to Steady Three-Dimensional Conduction Problems", ASME Paper No. 84-WA/HT-110, ASME Winter Annual Meeting, New Orleans, Louisiana, December 9-13, 1984.
18- Carslaw, H.S. and Jaeger, J.C., "Conduction of Heat in Solids", Oxford University Press, 2nd Edition, 1978.
19- Yovanovich, M.M., "General Expression for Circular Constriction Resistance for Arbitrary Flux Distribution", AIAA 13th Aerospace Science Meeting, American Institute of Aeronautics and Astronautics, Pasadena, CA, Jan. 20-22, 1975, Paper No. 75-188.
20- Turyk, P.J., and Yovanovich, M.M., "Transient Constriction Resistance for Elemental Flux Channels Heated by Uniform Flux Sources", ASME Winter Annual Meeting, Paper #84-HT-52, 1984.
21- Schneider, G.E., Strong, A.B., and Yovanovich, M.M., "Transient Thermal Response of Two Bodies Communicating through a Small Circular Contact Area", Int. J. Heat Mass Transfer, vol. 20, 1977, pp. 301-308.
22- Yovanovich, M.M., Negus, K.J., and Thompson, J.C., Transient Temperature Rise of Arbitrary Contacts with Uniform Flux by Surface Element Methods", AIAA 22nd Aerospace Sciences Meeting, American Institute of Aeronautics and Astronautics, Reno, Nevada, Jan., 1984, Paper No. AIAA-84-0397.

Nomenclature

- a amplitude of reciprocation (vm)
- A_{cn} contour area (m^2)
- A_{hfc} cross-sectional area of the HFC (m^2)
- A_{mic} micro-contact area (m^2)
- c_p specific heat (J kg^{-1} K^{-1})
- f frequency (s^{-1})
- k thermal conductivity of the material (W m^{-1} K^{-1})
- L half the length of the side of an asperity of a square cross section (μm)
- N_{integ} number of divisions per cycle, for numerical integration
- N_{nr} number of neighbouring heat sources in the near region
- P_a applied pressure (N m^{-2})
- P_c contact pressure over the area of the frictional heat source (N m^{-2})
- P_m flow pressure of the softer material (N m^{-2})
- $\tilde{q}$ sinusoidal heat flux over the micro-contact area (Wm^{-2})
- q_{fr} effective uniform heat flux over the far region (Wm^{-2})
- R_c thermal constriction resistance (K W^{-1})
- S spacing between two neighbouring micro-contacts (μm)
- t time (s)
- v velocity (ms^{-1})
- x,y,z cartesian coordinates

Greek Symbols

- α thermal diffusivity (m^2s^{-1})
- δ half the length of the side of the heat source under consideration (μm)
- θ temperature rise (K)
- λ half the length of the side of area over which the temperature is averaged (μm)
- μ coefficient of friction
- ρ mass density (kg m^{-3})
- σ initial time interval (Eq. 16)
- τ period of reciprocation (s)
- $\Delta\phi$ phase difference between the thermal constriction resistance and the frictional heat generation
- ω circular frequency of reciprocation (s^{-1})

Dimensionless parameters

- $\bar{A}$ amplitude parameter, $\bar{A}$= a/L
- f_a the ratio between the area of the starting heat source and the area over which the temperature is averaged, $f_a = 1/\bar{\lambda}^2$
- f_p the ratio between the contact pressure and flow pressure of the softer material, $f_p = p_c / p_m$
- Fo Fourier modulus, Fo= $\alpha\tau/L^2 = \alpha/f\,L^2$
- $R_{\bar{\psi}}$ the ratio between the thermal constriction parameters in the oscillating and stationary modes of motion, $R_{\bar{\psi}} = \bar{\psi}_{II}/\bar{\psi}_I$
- $\bar{t}$, $\tilde{t}$, $\Delta\tilde{t}$ dimensionless time parameters, $\bar{t} = \alpha t/L^2$, $\tilde{t} = t/\tau$, and $\Delta\tilde{t} = (t-t')/\tau$
- $\bar{x}$, $\bar{y}$, $\bar{z}$ dimensionless position co-ordinates, $\bar{x}$, $\bar{y}$, $\bar{z}$ = x/L, y/L, z/L
- γ the relative size of the contour area, $\gamma = \sqrt{[A_{cn}/A_{mic}]}$
- $\bar{\delta}$ characteristic length of the heat source, $\bar{\delta} = \delta/L$
- ε dimensionless constriction ratio (Eq. 1)
- Θ dimensionless temperature parameter, $\Theta = \theta\, c_p\rho / 4A\mu p_m$
- $\bar{\Theta}$ average temperature rise
- $\bar{\lambda}$ characteristic length of the area over which the temperature is averaged, heat source, $\bar{\lambda} = \lambda/L$
- ψ, $\bar{\psi}$ instantaneous and average value of the thermal constriction parameter, during the quasi-steady state cycle

Subscripts

- av average
- fr far region heat source
- I, II oscillatory and stationary modes of motion, respectively.
- ihs image heat source
- inst instantaneous
- m mean value
- nr near region heat source
- s point heat source, or stationary contact
- shs starting heat source

Symbols

- $fn\{...\}$ functional relationship
- $\equiv$ indicates

Appendix A:
Temperature Rise in a Semi-infinite Body Due to an Oscillatory, Sinusoidal Square Heat Source

At time t, the temperature rise θ at any point P(x,y,z) in a semi-infinite body due to an instantaneous point heat source $q(t=0)$ located on the surface at point $Q(x_s,y_s,0)$ is [18]:

$$\theta(x,y,z,t) = \frac{2q}{c_p\rho\,(4\pi\alpha t)^{3/2}}\ \exp\left(-\frac{r^2}{4\alpha t}\right) \qquad \text{(A1)}$$

where, $r^2 = (x-x_s)^2 + (y-y_s)^2 + z^2$, and α is the thermal diffusivity of the material. The temperature rise $\theta(x,y,z,t)$ due to the heat distributed over a square area $2\delta \times 2\delta$ located at (0,0,0), and omitted earlier at time t' is obtained by integrating Eq. A1 with respect to the space coordinates x_s and y_s:

$$\theta(x,y,z,t) = \frac{2}{c_p\rho}\int_{t'=0}^{t-t'} \left[\int_{x_s=-\delta}^{x_s=+\delta}\int_{y_s=-\delta}^{y_s=+\delta} q(t')\exp\left(\frac{F_{x,y,z,t}}{4\alpha(t-t')}\right)dx_s dy_s\right] \frac{dt'}{(4\alpha(t-t'))} \qquad \text{(A2)}$$

where:

$$F_{x,y,z,t} = \left[x - \int_{t'=0}^{t} v(t')dt' - x_s\right]^2 + [y-y_s]^2 + [z]^2 \qquad \text{(A3)}$$

$q(t')$ is the frictional heat: $q(t') = \mu\, p_c\, |v(t')|$, and $v(t')$ is the relative velocity of the oscillatory motion:

$$v(t') = \dot{x}(t') = a\,(2\pi f)\cos[(2\pi f)\,t'] \qquad \text{(A4)}$$

Integration of Eq. A2 results in the following expression:

$$\theta(\bar{x},\bar{y},\bar{z},\bar{t}) = \frac{\sqrt{\pi}}{8}\sqrt{Fo}\ f_p \int_{\Delta\bar{t}=0}^{\bar{t}-\bar{t}'} [F(\bar{z})]\,[F(\bar{x})]\,[F(\bar{y})]\,\frac{|\cos 2\pi(\bar{t}-\Delta\bar{t})|}{\sqrt{\Delta\bar{t}}}\,d\bar{t} \qquad \text{(A5)}$$

in terms of the dimensionless temperature parameter Θ:

$$\Theta = \frac{\theta k}{qL} = \frac{\theta k}{4(\mu p_m)(af)L} \qquad \text{(A6)}$$

and the following functions $F(\bar{x})$, $F(\bar{y})$, and $F(\bar{z})$:

$$F(\bar{z}) = \exp\left(-\frac{\bar{z}^2}{4\Delta\bar{t}\,Fo}\right)$$

$$F(\bar{x}) = \left(erf(A_{\bar{x}}) + erf(B_{\bar{x}})\right)$$

$$F(\bar{y}) = \left(erf(C_{\bar{y}}) + erf(D_{\bar{y}})\right) \qquad \text{(A7)}$$

$$A_{\bar{x}} = \frac{\bar{x} - \bar{A}\sin(2\pi\bar{t}) + A\sin 2\pi(\bar{t}-\Delta\bar{t}) + \bar{\delta}}{2\sqrt{[\Delta\bar{t}\,Fo]}}$$

$$B_{\bar{x}} = \frac{-\bar{x} + \bar{A}\sin(2\pi\bar{t}) - A\sin 2\pi(\bar{t}-\Delta\bar{t}) + \bar{\delta}}{2\sqrt{[\Delta\bar{t}\,Fo]}}$$

$$C_{\bar{y}} = \frac{\bar{\delta} + \bar{y}}{2\sqrt{\Delta\bar{t}\,Fo}}, \qquad D_{\bar{y}} = \frac{\bar{\delta} - \bar{y}}{2\sqrt{\Delta\bar{t}\,Fo}}$$

The dimensionless variables in Eq. A5 are defined as:
the amplitude parameter $\bar{A} = a/L$
the position co-ordinates $\bar{x}$, $\bar{y}$, $\bar{z}$ = x/L, y/L, z/L
the characteristic length of the heat source $\bar{\delta} = \delta/L$
Fourier modulus $Fo = \alpha\tau/L^2 = \alpha/f\,L^2$
the dimensionless time parameters $\bar{t} = \alpha t/L^2$, $\bar{t} = t/\tau$, and $\Delta\bar{t}=(t-t')/\tau$

The time τ is duration of the oscillation cycle, and the factor f_p in Eq. A5 is the ratio between the applied contact pressure and the flow pressure of the softer material, $f_p = p_a/p_m$. The dependence of the variables f_p and $\bar{\delta}$ (in Eq. A5) on the type of heat source is given in Table A1.

TABLE A1 VALUES OF THE VARIABLES f_p AND $\bar{\delta}$ FOR VARIOUS HEAT SOURCES

	starting heat source	image heat source	near region	far region
f_p	1	1	ε^2	ε^2
$\bar{\delta}$	1	1	$[\sqrt{N_{nr}}]/2\varepsilon$	∞